*International Journal of Thermophysics, Vol. 13, No. 6, 1992*

# Measurements of the Virial Coefficients and Equation of State of the Carbon Dioxide + Ethane System in the Supercritical Region

**L. A. Weber**[1]

*Received June 26, 1992*

Gas-phase densities of the system carbon dioxide + ethane were measured with a Burnett apparatus at 320 K and at pressures up to approximately 10 MPa. Measurements were made on systems having carbon dioxide mole fractions of 0, 0.25166, 0.49245, 0.73978, and 1. Second and third virial coefficients were determined for each composition, and the cross virial coefficients were calculated. Comparisons were made with other recent high-quality measurements on this system. For each mixture composition $P\rho T$ measurements were made on five isochores having densities within ±30% of the critical density. Temperatures varied from 288 to 320 K. The two-phase boundary was determined and estimates are given for $T_c$ and $P_c$ for each composition.

**KEY WORDS:** carbon dioxide; densities; equation of state; ethane; $P\rho T$; mixtures; virial coefficients.

## 1. INTRODUCTION

The importance of accurate metering in the natural gas industry has led to the expenditure of considerable effort in recent years toward the very accurate measurement of the properties of the pure components and their binary mixtures. Much of this work has been sponsored by the Gas Research Institute (GRI) of Chicago and the European Gas Research Group (GERG). The ultimate goal of these efforts is the development of a highly accurate equation of state for the calculation of the properties of multicomponent natural gas mixtures. Information on mixtures containing carbon dioxide also has useful application in enhanced oil recovery processes.

---

[1] Thermophysics Division, Chemical Science and Technology Laboratory, National Institute of Standards and Technology, Technology Administration, U.S. Department of Commerce, Gaithersburg, Maryland 20899, U.S.A.

We report here Burnett expansion measurements on pure $CO_2$ and pure ethane and three mixtures with $CO_2$ mole fractions of 0.25166, 0.49245, and 0.73978. All measurements were made at a temperature of 320 K, and for the mixtures the maximum densities were somewhat above critical. In addition, for the mixtures, isochoric $P\rho T$ measurements were made near the critical density downward in temperature to the vicinity of the two-phase boundary. We have estimated the location of the two-phase boundary in the critical region, and the estimated critical parameters $T_c$ and $P_c$ for each composition are given. From the Burnett data second and third virial coefficients were calculated for each system at 320 K, and the cross virials were derived for $CO_2 +$ ethane.

Even for very good gas-phase $P\rho T$ data, small uncertainties remain, which show up as uncertainties in the virial coefficients, particularly the third virial coefficients. These uncertainties are magnified when the cross virials are calculated for the mixture. When a correlation scheme is set up for a complex multicomponent mixture such as natural gas, certain higher-order interaction parameters must still be estimated. To reduce the uncertainties involved in this process, it is very useful to be able to minimize the uncertainties in the parameters for the major components,. which include $CO_2$ and ethane in this case. The assessment of the uncertainties is much more reliable when we are able to compare high-quality measurements from several different laboratories. There is a considerable body of literature on the virials of the pure components, $CO_2$ and ethane. The values have been compared by Brugge et al. [1], and we do not repeat those comparisons here. The literature on the $P\rho T$ data of the mixtures is limited, and we confine our comparisons to those with the results of Brugge et al. [1] and Jaeschke [2]. For the mixtures, the samples used here are the same ones used by Brugge et al., and thus we have a round-robin situation in which uncertainties due to composition are minimized. These samples have also been used by Diller et al. [3, 4] and Magee [5], who measured the viscosity and the specific heat.

In the next sections we give a description of the apparatus, the results, estimations of the virial coefficients and the critical parameters of the mixtures, and comparisons with the literature. We give some consideration to estimating the uncertainties in the derived virials and to comparing them with estimation schemes which have been proposed.

## 2. EXPERIMENTS

Measurements were made with the NIST Burnett apparatus, whose operating characteristics, estimated accuracies, and details of construction are well documented [6–8]. Recent measurements on alternative refrigerants [9–11] and their comparison with other high-quality work confirm the reliability of the results.

A heavy nickel Burnett cell and sensitive diaphragm-type pressure transducer, both gold-plated on the inside, are immersed in a circulated and thermostated oil bath. The transducer confines the thermostated volume and separates it from an argon-filled manifold which is connected to several pressure gauges at ambient temperatures. A motor-driven piston-type gas injector maintains the argon pressure equal to the sample pressure.

The system was operated automatically in the isochoric mode and semiautomatically in the Burnett gas expansion mode. For isochoric measurements, the diaphragm was balanced to within 100 Pa. For the Burnett expansions, balancing was done manually to within 10 Pa or less. The temperature of the oil bath was maintained and measured with an accuracy of 1–2 mK. All temperatures are given on the IPTS-68 temperature scale. Pressures are believed to be accurate to within 1 part in 10,000. The fact that they were generally reproducible within 200 Pa is a statement of the accuracy of the pressure and the temperature measuring systems. Densities are not measured, but they are calculated in the Burnett analysis. We estimate their accuracy to be within 0.02%. The cell constant (ratio of the final volume to the initial volume) was determined from expansions using helium gas, and it was considered to be fixed for the present measurements. We estimate that it has an uncertainty of 1 part in 25,000.

Data acquisition on each sample began with two series of Burnett expansions at 320 K. A gas-operated dead-weight gauge was used for the pressure measurements. For the three mixtures, measurements began at pressures in the vicinity of 10 MPa or at a density sightly above critical. After this, for the mixtures, a set of five isochores was measured at densities bracketing the critical density. Measurements were made downward in temperature, a short distance into the two-phase region. On the isochores, pressures were measured with an automated quartz spiral bourdon gauge. A pressure measurement on each isochore at 320 K allowed determination of its density.

Samples were prepared gravimetrically on a large-capacity balance having a resolution of 2.5 mg. The weighed amount of the pure gases varied from 380 to 1584 g. Since the samples had been used previously in several different laboratories, we checked the composition with our chromatograph to assure ourselves that fractionation had not occurred during sample withdrawal. The chromatograms agreed with the original sample preparation records to within the uncertainty of the chromatograph. For sample loading, the cylinders were heated to temperatures above the mixture critical temperatures, and all the intervening fill lines were also heated.

# 3. RESULTS

## 3.1. Burnett Data

The results of the Burnett expansion measurements, two series of expansions for each composition, are presented in Table I. Using a truncated virial equation,

$$P = RT\rho(1 + B_m\rho + C_m\rho^2) \tag{1}$$

where $B_m$ and $C_m$ are the mixture virial coefficients for a composition $x$, we analyzed the data and calculated densities with a parameter variation and linear analysis technique. These densities are given in Table I. For the purpose of this analysis we generally omitted data at pressures less than 0.3 MPa because of increasing relative error and data at densities greater than 2.5 mol · L$^{-1}$ (3.2 mol · L$^{-1}$ for $CO_2$) to minimize the effect of higher-order virials. Data with densities or pressures outside this range were calculated by making use of the cell constant, with a suitable small pressure correction. Standard deviations of the fits were of the order of 65–200 Pa. The virial coefficients found in this way are listed in columns 2 and 3 in Table III.

## 3.2. Isochoric Data

$P$, $T$ isochores were measured for each mixture composition at five densities around the mixture critical density. Pressures measured at 320 K were used to determine the densities. A small temperature correction to the density was made for the thermal expansion of the cell. The results are given in Table II.

**Table I.** Burnett Data for $CO_2$ + Ethane Mixtures at 320 K

| $P$ (MPa) | $\rho$ (mol · L$^{-1}$) | $P$ (MPa) | $\rho$ (mol · L$^{-1}$) |
|---|---|---|---|
| | $x_{CO_2} = 0$ | | |
| 0.34499 | 0.13251 | 0.47203 | 0.18268 |
| 0.60494 | 0.23613 | 0.82231 | 0.32555 |
| 1.04659 | 0.42080 | 1.40551 | 0.58015 |
| 1.76787 | 0.74990 | 2.32619 | 1.03387 |
| 2.85946 | 1.33637 | 3.62292 | 1.84245 |
| 4.27791 | 2.38154 | | |

**Table I.** (*Continued*)

| $P$ (MPa) | $\rho$ ($\mathrm{mol \cdot L^{-1}}$) | $P$ (MPa) | $\rho$ ($\mathrm{mol \cdot L^{-1}}$) |
|---|---|---|---|
| $X_{CO_2} = 0.25166$ | | | |
| 0.32944 | 0.12600 | 0.30674 | 0.11714 |
| 0.57939 | 0.22454 | 0.53987 | 0.20876 |
| 1.00817 | 0.40015 | 0.94103 | 0.37201 |
| 1.72122 | 0.71308 | 1.61145 | 0.66294 |
| 2.84040 | 1.27073 | | |
| 4.41436 | 2.26445 | 3.59393 | 1.70769 |
| 6.22016 | 4.03540 | 5.33822 | 3.04320 |
| 7.93121 | 7.19133 | 7.08808 | 5.42318 |
| | | 9.55686 | 9.66444 |
| $X_{CO_2} = 0.49245$ | | | |
| 0.19355 | 0.07337 | 0.13737 | 0.05196 |
| 0.34248 | 0.13073 | 0.24339 | 0.09257 |
| 0.60279 | 0.23293 | 0.43032 | 0.16494 |
| 1.05089 | 0.41501 | 0.75502 | 0.29388 |
| 1.80112 | 0.73944 | 1.30882 | 0.52361 |
| 2.99390 | 1.31748 | 2.22040 | 0.93293 |
| 4.71720 | 2.34742 | 3.62487 | 1.66225 |
| 6.81158 | 4.18244 | 5.53807 | 2.96166 |
| | | 7.66365 | 5.27684 |
| | | 10.19437 | 9.40186 |
| $X_{CO_2} = 0.73978$ | | | |
| 0.30598 | 0.11647 | 0.41792 | 0.15983 |
| 0.53986 | 0.20755 | 0.73475 | 0.28482 |
| 0.94539 | 0.36986 | 1.27794 | 0.50757 |
| 1.63236 | 0.65911 | 2.18045 | 0.90450 |
| 2.74904 | 1.17456 | 3.59540 | 1.61184 |
| 4.42936 | 2.09311 | 5.58426 | 2.87236 |
| 6.61777 | 3.72992 | 7.88295 | 5.11872 |
| 8.89209 | 6.64669 | 10.20559 | 9.12188 |
| 12.19874 | 11.84417 | | |
| $X_{CO_2} = 1.0$ | | | |
| 0.13927 | 0.36510 | 0.46021 | 0.09888 |
| 0.64337 | 0.24819 | 0.80847 | 0.31405 |
| 1.12343 | 0.44229 | 1.40399 | 0.55965 |
| 1.93007 | 0.78820 | 2.38841 | 0.99734 |
| 3.22049 | 1.40462 | 3.91531 | 1.77732 |
| 5.09921 | 2.50311 | 6.00609 | 3.16729 |

**Table II.** Isochoric $P\rho T$ Data for the $CO_2$ + Ethane System

| $T$ (K) | $P$ (MPa) | $\rho$ ($mol \cdot L^{-1}$) |
|---|---|---|
| | $X_{CO_2} = 0.25166$ | |
| 320.007 | 8.9707 | 8.9511 |
| 318.129 | 8.6807 | 8.9518 |
| 313.132 | 7.9132 | 8.9537 |
| 308.176 | 7.1599 | 8.9555 |
| 303.141 | 6.4070 | 8.9474 |
| 298.171 | 5.6836 | 8.9593 |
| 297.161 | 5.5407 | 8.9597 |
| 296.903 | 5.5044 | 8.9598 |
| 296.637 | 5.4669 | 8.9599 |
| 296.403 | 5.4344 | 8.9600 |
| 296.190 | 5.4052 | 8.9601 |
| 295.888 | 5.3635 | 8.9602 |
| 295.674 | 5.3345 | 8.9602 |
| 295.415 | 5.2998 | 8.9603 |
| 295.137 | 5.2704 | |
| 294.149 | 5.1654 | |
| 293.153 | 5.0615 | |
| | | |
| 319.998 | 7.6184 | 6.5229 |
| 318.126 | 7.4380 | 6.5234 |
| 313.137 | 6.9560 | 6.5248 |
| 308.170 | 6.4745 | 6.5261 |
| 303.154 | 5.9862 | 6.5275 |
| 298.128 | 5.4929 | 6.5289 |
| 297.158 | 5.3963 | 6.5292 |
| 296.906 | 5.3711 | 6.5292 |
| 296.638 | 5.3443 | 6.5293 |
| 296.399 | 5.3200 | |
| 296.193 | 5.2986 | |
| 295.891 | 5.2675 | |
| 295.682 | 5.2453 | |
| 295.418 | 5.2184 | |
| 295.140 | 5.1893 | |
| 294.141 | 5.0865 | |
| 293.142 | 4.9849 | |
| | | |
| 320.007 | 9.5580 | 9.6612 |
| 318.131 | 9.2266 | 9.6620 |
| 313.163 | 8.3546 | 0.6640 |
| 308.174 | 7.4882 | 9.6660 |
| 303.150 | 6.6300 | 9.6680 |
| 298.138 | 5.7957 | 9.6701 |

Table II. (*Continued*)

| $T$ (K) | $P$ (MPa) | $\rho$ ($\mathrm{mol \cdot L^{-1}}$) |
|---|---|---|
| 297.175 | 5.6391 | 9.6705 |
| 296.657 | 5.5557 | 9.6707 |
| 296.412 | 5.5165 | 9.6708 |
| 296.134 | 5.4722 | 9.6709 |
| 295.175 | 5.3208 | 9.6713 |
| 294.142 | 5.1754 | |
| 293.144 | 5.0706 | |
| | | |
| 320.005 | 8.4795 | 8.2264 |
| 318.129 | 8.2278 | 8.2270 |
| 313.151 | 7.5625 | 8.2288 |
| 308.167 | 6.9020 | 8.2305 |
| 303.147 | 6.2450 | 8.2322 |
| 298.136 | 5.6035 | 8.2340 |
| 297.171 | 5.4829 | 8.2343 |
| 296.923 | 5.4523 | 8.2344 |
| 296.655 | 5.4193 | 8.2345 |
| 296.411 | 5.3894 | 8.2346 |
| 296.130 | 5.3555 | 8.2346 |
| 295.904 | 5.3297 | |
| 295.702 | 5.3093 | |
| 295.384 | 5.2742 | |
| 295.178 | 5.2532 | |
| 294.143 | 5.1433 | |
| 293.143 | 5.0395 | |
| | | |
| 320.007 | 7.9409 | 7.2072 |
| 318.147 | 7.7355 | 7.2078 |
| 313.156 | 7.1852 | 7.2093 |
| 308.177 | 6.6371 | 7.2108 |
| 303.170 | 6.0876 | 7.2123 |
| 298.147 | 5.5387 | 7.2138 |
| 297.179 | 5.4331 | 7.2141 |
| 296.930 | 5.4060 | 7.2142 |
| 296.662 | 5.3769 | 7.2143 |
| 296.419 | 5.3504 | |
| 296.139 | 5.3211 | |
| 295.907 | 5.2966 | |
| 295.702 | 5.2750 | |
| 295.392 | 5.2422 | |
| 295.176 | 5.2194 | |
| 294.133 | 5.1109 | |
| 293.147 | 5.0099 | |

**Table II.** (*Continued*)

| $T$ (K) | $P$ (MPa) | $\rho$ ($\mathrm{mol \cdot L^{-1}}$) |
|---|---|---|
| | $X_{CO_2} = 0.49245$ | |
| 319.983 | 9.2725 | 7.9949 |
| 318.168 | 9.0453 | 7.9955 |
| 313.158 | 8.4177 | 7.9972 |
| 308.194 | 7.7974 | 7.9989 |
| 303.171 | 7.1704 | 8.0005 |
| 298.154 | 6.5462 | 8.0022 |
| 297.178 | 6.4252 | 8.0026 |
| 296.162 | 6.2990 | 8.0029 |
| 295.166 | 6.1757 | 8.0032 |
| 294.106 | 6.0443 | 8.0036 |
| 293.143 | 5.9253 | 8.0039 |
| 292.178 | 5.8062 | 8.0042 |
| 291.168 | 5.6815 | 8.0046 |
| 290.163 | 5.5592 | |
| 289.173 | 5.4407 | |
| 288.166 | 5.3221 | |
| | | |
| 320.037 | 9.0003 | 7.5120 |
| 318.174 | 8.7866 | 7.5126 |
| 313.167 | 8.2120 | 7.5142 |
| 308.136 | 7.6337 | 7.5158 |
| 303.170 | 7.0626 | 7.5173 |
| 298.157 | 6.4850 | 7.5189 |
| 297.130 | 6.3658 | 7.5192 |
| 296.166 | 6.2545 | 7.5195 |
| 295.162 | 6.1385 | 7.5198 |
| 294.109 | 6.0162 | 7.5202 |
| 293.139 | 5.9038 | |
| 292.176 | 5.7914 | |
| 291.168 | 5.6731 | |
| 290.153 | 5.5506 | |
| 289.174 | 5.4336 | |
| 288.160 | 5.3151 | |
| | | |
| 319.981 | 8.7318 | 7.0496 |
| 318.167 | 8.5412 | 7.0501 |
| 313.164 | 8.0139 | 7.0516 |
| 308.156 | 7.4847 | 7.0531 |
| 303.169 | 6.9556 | 7.0546 |
| 298.153 | 6.4204 | 7.0561 |
| 297.175 | 6.3154 | 7.0564 |
| 296.168 | 6.2070 | 7.0567 |

Table II. (*Continued*)

| $T$ (K) | $P$ (MPa) | $\rho$ ($\mathrm{mol \cdot L^{-1}}$) |
|---|---|---|
| 295.156 | 6.0979 | 7.0570 |
| 294.103 | 5.9840 | 7.0573 |
| 293.143 | 5.8794 | 7.0575 |
| 292.180 | 5.7741 | 7.0578 |
| 291.168 | 5.6619 | 7.0581 |
| 290.149 | 5.5410 | |
| 289.172 | 5.4255 | |
| 288.158 | 5.3072 | |
| 287.135 | 5.1905 | |
| | | |
| 319.976 | 9.5360 | 8.4322 |
| 318.166 | 9.2909 | 8.4328 |
| 313.160 | 8.6138 | 8.4346 |
| 308.133 | 7.9364 | 8.4364 |
| 303.166 | 7.2704 | 8.4382 |
| 298.154 | 6.6029 | 8.4399 |
| 297.176 | 6.4734 | 8.4403 |
| 296.180 | 6.3416 | 8.4406 |
| 295.158 | 6.2071 | 8.4410 |
| 294.105 | 6.0689 | 8.4414 |
| 293.140 | 5.9428 | 8.4417 |
| 292.175 | 5.8176 | 8.4420 |
| 291.165 | 5.6878 | 8.4424 |
| 290.151 | 5.5633 | |
| 289.171 | 5.4456 | |
| 288.156 | 5.3262 | |
| 287.135 | 5.2085 | |
| | | |
| 319.976 | 9.1402 | 7.7693 |
| 318.095 | 8.9142 | 7.7699 |
| 311.435 | 8.1128 | 7.7721 |
| 295.153 | 6.1555 | 7.7774 |
| 293.148 | 5.9146 | 7.7781 |
| 292.127 | 5.7919 | 7.7784 |
| 291.922 | 5.7673 | 7.7785 |
| 291.675 | 5.7375 | 7.7785 |
| 291.417 | 5.7063 | 7.7786 |
| 291.169 | 5.6763 | 7.7787 |
| 290.907 | 5.6447 | 7.7788 |
| 290.666 | 5.6153 | 7.7789 |
| 290.409 | 5.5843 | 7.7789 |
| 290.152 | 5.5535 | 7.7790 |
| 289.175 | 5.4369 | |
| 288.161 | 5.3183 | |

**Table II.** (*Continued*)

| $T$ (K) | $P$ (MPa) | $\rho$ ($\mathrm{mol \cdot L^{-1}}$) |
|---|---|---|
| | $C_{CO_2} = 0.73978$ | |
| 319.982 | 12.1947 | 11.8474 |
| 318.121 | 11.7713 | 11.8483 |
| 313.174 | 10.6784 | 11.8508 |
| 308.143 | 9.5684 | 11.8533 |
| 303.164 | 8.4836 | 11.8558 |
| 298.158 | 7.4146 | 11.8583 |
| 297.128 | 7.1981 | 11.8588 |
| 296.168 | 6.9975 | 11.8593 |
| 295.167 | 6.7909 | 11.8598 |
| 294.894 | 6.7345 | 11.8599 |
| 294.649 | 6.6843 | 11.8600 |
| 294.392 | 6.6317 | 11.8601 |
| 294.199 | 6.5921 | 11.8602 |
| 293.891 | 6.5294 | 11.8604 |
| 293.664 | 6.4840 | 11.8605 |
| 293.433 | 6.4371 | 11.8606 |
| 293.154 | 6.3806 | 11.8608 |
| 292.175 | 6.1864 | |
| 291.162 | 6.0167 | |
| | | |
| 319.975 | 10.2022 | 9.1229 |
| 318.164 | 9.9372 | 9.1236 |
| 313.154 | 9.2030 | 9.1255 |
| 308.183 | 8.4762 | 9.1274 |
| 303.165 | 7.7445 | 9.1294 |
| 298.152 | 7.0166 | 9.1313 |
| 297.176 | 6.8748 | 9.1316 |
| 296.161 | 6.7285 | 9.1320 |
| 295.159 | 6.5839 | 9.1324 |
| 294.887 | 6.5446 | 9.1325 |
| 294.647 | 6.5103 | 9.1326 |
| 294.389 | 6.4730 | 9.1327 |
| 294.193 | 6.4449 | 9.1328 |
| 293.882 | 6.4000 | 9.1329 |
| 293.665 | 6.3676 | 9.1330 |
| 293.426 | 6.3344 | 9.1331 |
| 293.151 | 6.2953 | 9.1332 |
| 292.174 | 6.1565 | |
| 291.161 | 6.0161 | |
| | | |
| 319.980 | 9.7371 | 8.2512 |
| 318.175 | 9.5071 | 8.2518 |

Table II. (*Continued*)

| $T$ (K) | $P$ (MPa) | $\rho$ ($\mathrm{mol \cdot L^{-1}}$) |
|---|---|---|
| 313.159 | 8.8678 | 8.2536 |
| 308.125 | 8.2244 | 8.2553 |
| 303.165 | 7.5885 | 8.2570 |
| 298.183 | 6.9470 | 8.2588 |
| 297.147 | 6.8129 | 8.2591 |
| 296.172 | 6.6863 | 8.2595 |
| 295.175 | 6.5566 | 8.2598 |
| 294.903 | 6.5213 | 8.2599 |
| 294.663 | 6.4896 | 8.2600 |
| 294.405 | 6.4562 | 8.2601 |
| 294.209 | 6.4302 | 8.2601 |
| 293.903 | 6.3898 | 8.2602 |
| 293.672 | 6.3598 | 8.2603 |
| 293.430 | 6.3276 | 8.2604 |
| 293.158 | 6.2915 | 8.2605 |
| 292.180 | 6.1566 | |
| 291.172 | 6.0165 | |
| | | |
| 319.972 | 10.7307 | 9.9743 |
| 318.167 | 10.4261 | 9.9751 |
| 313.158 | 9.5832 | 9.9772 |
| 308.133 | 8.7421 | 9.9793 |
| 303.168 | 7.9182 | 9.9814 |
| 298.154 | 7.0968 | 9.9835 |
| 297.128 | 6.9307 | 9.9839 |
| 296.163 | 6.7751 | 9.9843 |
| 295.168 | 6.6161 | 9.9847 |
| 294.890 | 6.5715 | 9.9848 |
| 294.651 | 6.5336 | 9.9849 |
| 294.393 | 6.4931 | 9.9850 |
| 294.201 | 6.4626 | 9.9851 |
| 293.896 | 6.4144 | 9.9852 |
| 293.667 | 6.3787 | 9.9853 |
| 293.427 | 6.3411 | 9.9854 |
| 293.154 | 6.2989 | 9.9855 |
| 292.178 | 6.1570 | |
| 291.167 | 6.0167 | |
| | | |
| 319.981 | 9.2511 | 7.3101 |
| 318.171 | 9.0550 | 7.3107 |
| 313.147 | 8.5077 | 7.3122 |
| 308.134 | 7.9581 | 7.3137 |
| 303.176 | 7.4101 | 7.3153 |
| 298.160 | 6.8486 | 7.3168 |

Table II. (*Continued*)

| $T$ (K) | $P$ (MPa) | $\rho$ (mol · L$^{-1}$) |
|---|---|---|
| 297.131 | 6.7321 | 7.3171 |
| 296.158 | 6.6212 | 7.3174 |
| 295.146 | 6.5055 | 7.3177 |
| 294.938 | 6.4815 | 7.3178 |
| 294.646 | 6.4480 | 7.3179 |
| 294.389 | 6.4181 | 7.3180 |
| 294.192 | 6.3953 | 7.3180 |
| 293.893 | 6.3606 | 7.3181 |
| 293.662 | 6.3336 | 7.3182 |
| 293.418 | 6.3051 | 7.3183 |
| 293.144 | 6.2731 | 7.3183 |
| 292.171 | 6.1523 | |
| 291.158 | 6.0140 | |

The isochores were differenced to ensure smoothness and plotted to find their intersections with the two-phase boundaries. The general location of the data is shown in Fig. 1, where they are superimposed on a figure taken from Ohgaki and Katayama [12]. The $\rho$–$T$ loci of the two-phase boundaries are shown in Figs. 2a–c. In Fig. 2c for the $CO_2$-rich mixture,

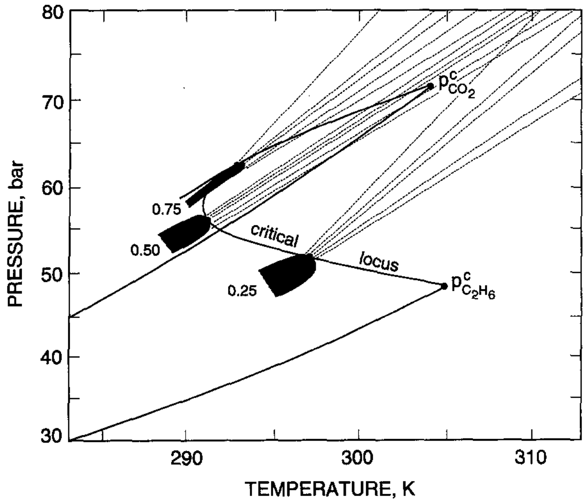

Fig. 1. Critical locus of the $CO_2$ + ethane system showing the location of the two-phase boundaries and experimental isochores.

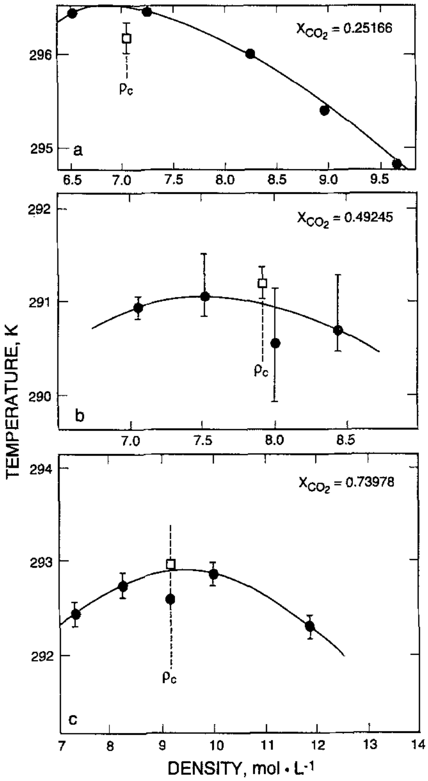

**Fig. 2.** The $\rho$–$T$ loci of the two-phase boundaries found from isochore intersections; (□) critical points from Abacci et al. [21].

the curve has a pure fluid-like symmetry because of its proximity to the azeotropic composition, $x \approx 0.72$. In Fig. 2b for the nearly equimolar composition, the data are not definitive, but the curve appears to be nearly symmetric because $T_c$ is near the temperature minimum of the critical locus for this system. The ethane-rich composition in Fig. 2a displays the asymmetry more typical for a mixture. Figure 3a–c show the boundaries in $P$–$T$ coordinates along with the estimated critical locus, shown in Fig. 1. Our estimated values for the critical pressures and temperatures of the mixtures are given in Table IV. In Table II the entires with no densities are data inside the two-phase region.

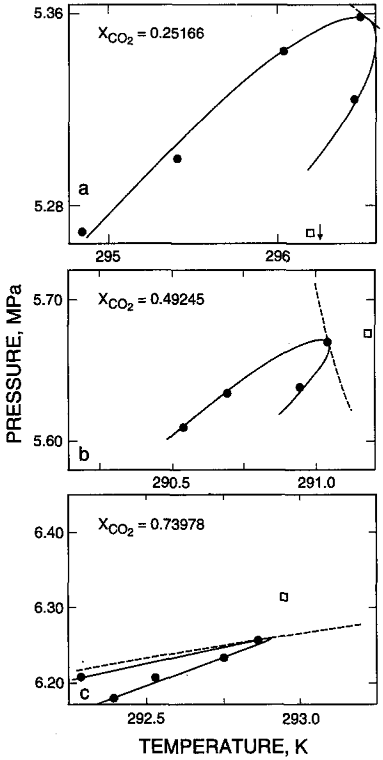

**Fig. 3.** Two-phase boundaries in *P–T* coordinates; (□) critical points from Abacci et al. [21].

## 3.3. Virial Coefficients

The mixture virial coefficients found from the analysis of the isotherm for each isopleth are given in the second and third columns in Table III. The statistics of the analysis also provided an estimate of the uncertainty of each coefficient, but we do not give these estimates here because we have found that they are often too optimistic, possibly by as much as a factor of three for highly precise $P\rho T$ data, which have a correlation coefficient very nearly equal to one. Rather, they have been estimated by the use of a empirical resampling technique which makes use of the estimated uncertainties in the experimental pressures. These estimates are also given in columns 2 and 3 in Table III. They are seen to vary somewhat from one isopleth to another, since they depend on the precision and range of the

Table III. Virial Coefficients. $B$ and $C$, of the $CO_2$ + Ethane System

| | Isopleth | | Surface, Eqs. (1)–(3) | |
|---|---|---|---|---|
| $X_{CO_2}$ | $B$ ($10^3$ L · mol$^{-1}$) | $C$ ($10^6$ L$^2$ · mol$^{-2}$) | $B$ ($10^3$ L · mol$^{-1}$) | $C$ ($10^6$ L$^2$ · mol$^{-2}$) |
| 0 | −159.38 | 9641 | −159.39 | 9650 |
| | ±0.17 | ±68 | | |
| 0.25166 | −135.71 | 7799 | −135.50 | 7770 |
| | ±0.17 | ±59 | | |
| 0.49245 | −118.97 | 6271 | −119.00 | 6283 |
| | ±0.07 | ±30 | | |
| 0.73978 | −108.57 | 5158 | −108.52 | 5130 |
| | ±0.23 | ±110 | | |
| 1 | −104.58 | 4381 | −104.59 | 4385 |
| | ±0.11 | ±33 | | |
| $B_{12}$ | −105.40 | | −105.17 | |
| | ±0.20 | | | |
| $C_{112}$ | | 5031 | 5005 | |
| | | ±170 | | |
| $C_{122}$ | | 6999 | 6963 | |
| | | ±170 | | |

data in each case. For further estimation, we have assumed $\delta B$ and $\delta C$ to be $\pm 0.15 \times 10^{-3}(\mathrm{L \cdot mol^{-1}})$ and $\pm 100 \times 10^{-6}(\mathrm{L \cdot mol^{-1}})^2$, respectively.

The mixture virial coefficients may be calculated from the mixing rules,

$$B_m = \sum_i \sum_j x_i x_j B_{ij} \tag{2}$$

$$C_m = \sum_i \sum_j \sum_k x_i x_j x_k C_{ijk} \tag{3}$$

with $B_m$ and $C_m$ being the virial coefficients of the mixtures and $B_{ij}$ and $C_{ijk}$ being the pure fluid virials, $B_{11}$, $B_{22}$, $C_{111}$, and $C_{222}$, and the cross virials,

Table IV. Critical Pressures and Temperatures of $CO_2$ + Ethane Mixtures

| $X_{CO_2}$ | $T_c$ (K) | $P_c$ (MPa) |
|---|---|---|
| 0.25166 | 296.55 | 5.357 |
| 0.49245 | 291.05 | 5.668 |
| 0.73978 | 292.90 | 6.260 |

$B_{12}$, $C_{112}$, and $C_{122}$. From the values of $B_m$ and $C_m$ given in Table III, we can calculate the cross virials via Eqs. (2) and (3). The results are given in the lower part of the table. Alternatively, we may use a combination of Eqs. (1)–(3) to represent all of the data in Table I (within the pressure and density limits given above) simultaneously. This seven-parameter function, $P = P(T, \rho, x)$, fits the experimental data very well and has a standard deviation of 0.18 kPa, or 0.010% in the compressibility factor, $Z$. The resulting parameters are given in columns 4 and 5 in Table III. Comparison of the virials in Table III shows that the two methods of obtaining the coefficients are in excellent agreement. Because of the correlation between $B$ and $C$, the latter method (columns 4 and 5) is probably preferable since this set of parameters is completely consistent and capable of reproducing the surface at any composition with maximum accuracy. The calculations on the isopleths provide an easier way to estimate the uncertainties of each coefficient.

## 4. COMPARISONS

### 4.1. Virial Coefficients

Dymond and Smith [13] define "Class I" data as those which produce second virial coefficients with an estimated precision $<2\%$ or $<1 \times 10^{-3}\,\mathrm{L \cdot mol^{-1}}$, whichever is greater. For this system we have identified two experimental references which meet or exceed this definition, and we limit our comparisons to these two. They are Brugge et al. [1], which also makes use of the pure component measurements of Holste et al. [14, 15], and Jaeschke [2]. The former are also Burnett measurements, while the latter reference utilizes a Burnett-coupled optical interferometer. We also include here a comparison with the GERG correlation [16]. A detailed comparison is given in Table V, where the quantities $|\Delta B|$ and $|\Delta C|$ are the differences from our measured values on isopleths in Table III. We see that the agreement with the other recent experimental work is excellent, with the average $\Delta B$ being considerably less than $1 \times 10^{3}\,\mathrm{L \cdot mol^{-1}}$, and the average $\Delta C$ also is very small. The cross virials also agree remarkably well, and in general, the overall agreement is within the uncertainties given in Table III. The disagreement with the GERG correlation is a little larger but still small by most standards and generally within their estimates of uncertainty.

Further comparisons are made in Figs. 4a and b. In Fig. 4 we have plotted differences in the quantity,

$$(Z-1)/\rho = B + C\rho \qquad (4)$$

**Table V.** Comparison of Our Results with Literature Values; $\lvert \Delta B \rvert$ and $\lvert \Delta C \rvert$ are Differences from Our Values on Isopleths

| | $10^3$ L·mol$^{-1}$ | | $10^6$ L$^2$·mol$^{-2}$ | | |
|---|---|---|---|---|---|
| $X_{CO_2}$ | $B$ | $\lvert \Delta B \rvert$ | $C$ | $\lvert \Delta C \rvert$ | |
| Brugge et al. [1] | | | | | |
| 0 | −159.36 | 0.02 | 9652 | 11 | |
| 0.25166 | −135.66 | 0.05 | 7796 | 3 | $B_{12} = -105.70$ |
| 0.49245 | −119.32 | 0.35 | 6321 | 50 | $C_{112} = 4912$ |
| 0.73978 | −108.73 | 0.16 | 5176 | 18 | $C_{122} = 7166$ |
| 1 | −104.70 | 0.12 | 4423 | 42 | |
| ⟨ ⟩ | | 0.14 | | 25 | |
| Jaeschke [2] | | | | | |
| 0 | −159.01 | 0.37 | 9496 | 145 | |
| 0.25166 | −136.18 | 0.47 | | | |
| 0.49245 | −120.06 | 1.09 | | | $B_{12} = -107.58$ |
| 0.73978 | −109.32 | 0.75 | | | |
| 1 | −104.40 | 0.18 | 4299 | 82 | |
| ⟨ ⟩ | | 0.57 | | 114 | |
| GERG [16] | | | | | |
| 0 | −159.78 | 0.40 | 9825 | 184 | |
| 0.25166 | −136.51 | 0.80 | 8147 | 348 | $B_{12} = -107.15$ |
| 0.49245 | −120.26 | 1.29 | 6777 | 506 | $C_{112} = 5709$ |
| 0.73978 | −109.69 | 1.12 | 5610 | 452 | $C_{122} = 7436$ |
| 1 | −105.28 | 0.70 | 4644 | 263 | |
| ⟨ ⟩ | | 0.86 | | 351 | |

which displays the data at lower densities in greater detail. The differences shown are between our data, used to calculate the left side of Eq. (4), and the right side, which uses the values of $B$ and $C$ from the indicated reference. All of the experimental data are seen to agree within ±0.02%. The calculated values from GERG [16] in Fig. 4a agree a little less well because they are based mainly on the work of Michels and Michels [17], which differs somewhat from our results for $CO_2$.

In Figs. 5a–c we have used a five-parameter, virial-type power series to represent all of the data for each composition in Table I. These figures demonstrate our precision and show how our results compare with the other references. We see that, although there are some obvious systematic differences, the results agree to within 0.1% up to a pressure of about 6 MPa. Agreement to this pressure is more than sufficient for natural-gas calculations, where the partial pressures of these two components are

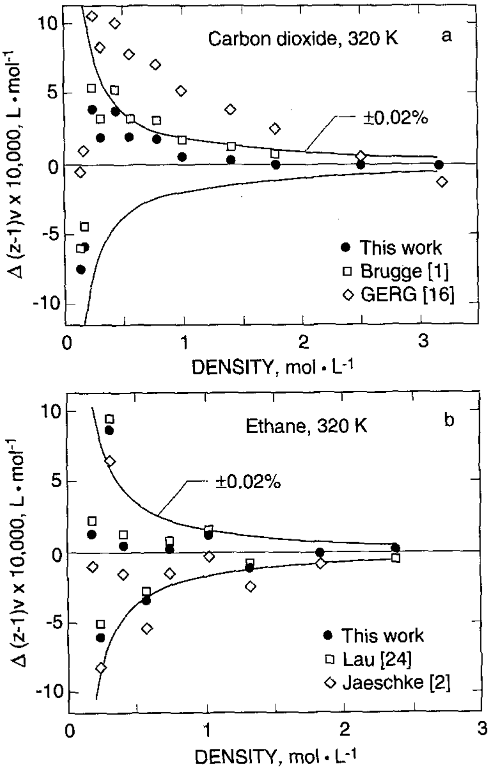

**Fig. 4.** Comparisons with the literature for the pure components.

always far less. Also shown in Fig. 5 are the results of Lau [24], who used a direct weighing apparatus. These results agree at the 0.1 % level, and they extend to higher pressures than shown here.

Figure 6 is a more detailed study of Fig. 5b for the equimolar mixture. It shows the effects of different ways of treating the data and the effects of some experimental parameters. Curve 1 is the GERG curve and curve 2 uses the virial coefficients from the data of Brugge et al., shown in Fig. 5b. The small systematic trend shown for curve 2 results mainly from a difference of only 0.35 $\mathrm{cm}^3 \cdot \mathrm{mol}^{-1}$ between the second virial coefficients. Curves 3–7 illustrate the effects of different ways of fitting our data. Curve 3 is a two-parameter fit to the data up to a maximum pressure of 3.0 MPa; curve 4 fits data to 3.6 Mpa; and curves 5 and 6 fit data to 4.8 MPa, with and without a small pressure correction to the cell constant. Curve 7 uses three parameters to fit data up to 7.5 MPa. Curve 8 illustrates the effect of an error in the cell constant of 1 part in 10,000. These curves show the

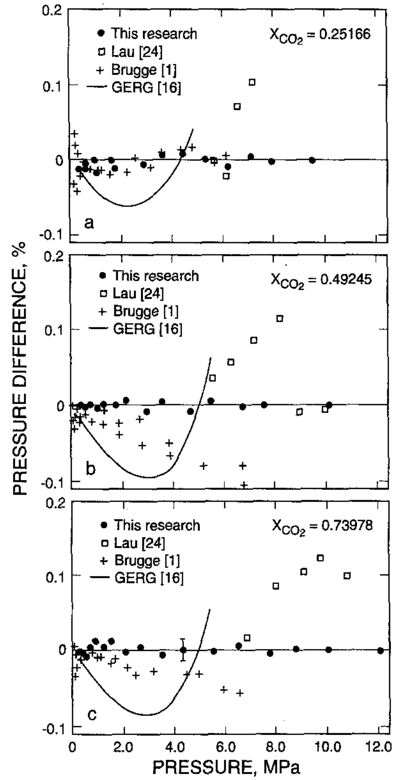

**Fig. 5.** Comparisons with the literature for the three mixture compositions.

effect of the correlation between the value of *B* and that of *C* and demonstrate the fact that two-parameter fits should be extrapolated upward in pressure only with great caution. For errors in the cell constant of the size expected here, the effect is relatively small.

McGregor et al. [18] have suggested a relationship between the third virial coefficients of mixtures which has some theoretical foundation,

$$C_{112} - C_{122} = (C_{111} - C_{222})/3 \tag{5}$$

This relationship is particularly useful in reducing the number of parameters and constraining the coefficients when fitting $P\rho T$ data which are sparse or which are of lower quality. Comparing Eq. (5) with our results in Table III, we see that our values for the cross virials fail to satisfy the equation by only about $200 \times 10^{-6}$ $(\mathrm{L \cdot mol^{-1}})^2$, an amount within their combined uncertainties. If we refit our Burnett data, using

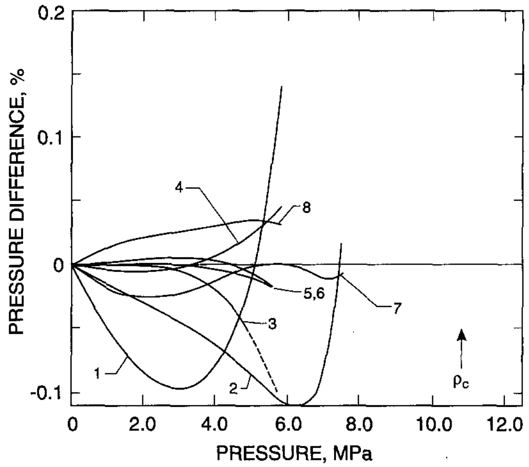

**Fig. 6.** Effects of different ways of fitting the data. See text for complete explanation.

Eqs. (1)–(3) and incorporating the above constraint on the cross third virials, there is essentially no degradation in the quality of the fit. The cross third virials obtained in this way are $C_{112} = 5151 \times 10^{-6}$ and $C_{122} = 6901 \times 10^{-6}$ ($L^2 \cdot mol^{-2}$), while all of the other coefficients are virtually unchanged. Thus we can say that our data are consistent with Eq. (5).

In cases where interaction third virials have not been measured, one method for their estimation which has been suggested [16] is the relationship

$$C_{iij} = \xi_{iij}(C_{iii}C_{iii}C_{jjj})^{1/3} \tag{6}$$

which relates them to those of the pure components. This method is more restrictive than Eq. (5), and the $\xi$'s must be estimated by some means, but this technique can be useful where few or no mixture data are available. If we apply Eq. (6) to our data [using Eq. (5)], we obtain $\xi_{112} = 0.90 \pm 0.02$ and $\xi_{122} = 0.93 \pm 0.02$. We may say that these values are the same within their uncertainties. We might also note that these $\xi \approx (1 - k_{ij})$ found by Holste et al. [14] for this system, where the $k_{ij}$ was found from

$$T_{cij} = (T_{ci}T_{cj})^{1/2}(1 - k_{ij}) \tag{7}$$

The criterion for determining $k_{ij}$ or $T_{cij}$ was the agreement between their experimental cross second virials and those calculated from the Tsonopoulos [19] modification of the method of Pitzer and Curl [20], which makes use of the reduced temperature. We should be cautious, however, about observing too many relationships from such a limited case study.

### 4.2. Isochoric Data

We are not aware of the existence of any other $P\rho T$ data for the mixtures in the region or our isochoric data. However, the isochoric data allowed us to determine three points on the critical locus of the $CO_2$ + ethane system. This locus has been measured a number of times, and a comprehensive survey and correlation of the results are given by Abbaci et al. [21]. The critical points for these compositions, from their correlation, are also plotted in Figs. 2 and 3. Our results agree reasonably well, with only the difference in $P_c$ for $x = 0.25$ disagreeing by about 2%. We estimate the uncertainty in our critical temperature to be 0.2–0.4 K. Jin et al. [22] have modeled this system with a crossover model based on an idea of Griffiths and Wheeler [23]. Their model fits our isochoric data with a standard deviation of 0.6% in pressure. The data were also fit about equally well by a NIST mixture property database program [25].

## 5. CONCLUSIONS

We have made an accurate determination of the virial coefficients of the $CO_2$ + ethane system at 320 K and have compared our results with the best available measurements in the literature. In addition, we have made careful and realistic estimates of the uncertainties in the coefficients. Our values agree with the literature values generally within their estimated uncertainties, and the comparisons at 320 K contribute information about the confidence limit for the literature values at other temperatures. We have made isochoric $P\rho T$ measurements on three mixture compositions in the supercritical region and have determined estimates for their critical pressures and temperatures.

## ACKNOWLEDGMENTS

The mixtures were prepared by W. M. Haynes. This work was carried out with support from the Gas Research Institute.

## REFERENCES

1. H. B. Brugge, C.-A. Hwang, W. J. Rogers, J. C. Holste, K. R. Hall, W. Lemming, G. J. Esper, K. N. Marsh, and B. E. Gammon, *Physica A* **156**:382 (1989).
2. M. Jaeschke, *Int. J. Thermophys.* **8**:81 (1987).

3. D. E. Diller and J. E. Ely, *High Temp. High Press.* **21**:613 (1989).
4. D. E. Diller, L. J. Van Poolen, and F. V. dos Santos, *J. Chem. Eng. Data* **33**:460 (1988).
5. J. W. Magee, in press.
6. M. Waxman and J. R. Hastings, *J. Res. Natl. Bur. Stand.* **75**C:165 (1971).
7. M. Waxman, H. A. Davis, M. Horowitz, and B. Everhart, *Rev. Sci. Instrum.* **55**:1467 (1984).
8. D. Linsky, J. M. H. Levelt Sengers, and H. A. Davis, NBS Tech. Note 1051 (1982).
9. L. A. Weber, *Int. J. Thermophys.* **10**:617 (1989).
10. L. A. Weber, *J. Chem. Eng. Data* **35**:237 (1990).
11. L. A. Weber, Proc. XVIIIth Int. Congr. Refrig., No. 69, Montreal (1991), ISBN 2-9802798-0-3.
12. K. Ohgaki and T. Katayama, *Fluid Phase Equil.* **1**:27 (1977).
13. J. H. Dymond and E. B. Smith, *The Virial Coefficients of Pure Gases and Mixtures* (Oxford University Press, Oxford, 1980).
14. J. C. Holste, J. G. Young, P. T. Eubank, and K. R. Hall, *AIChE J.* **28**:807 (1982).
15. J. C. Holste, K. R. Hall, P. T. Eubank, G. Esper, M. Q. Watson, W. Warowny, D. M. Bailey, J. G. Young, and M. T. Bellomy, *J. Chem. Thermodyn.* **19**:1233 (1987).
16. Groupe Européen de Recherhes Gazières (GERG), TM2, M. Jaeschke, Convenor (1988).
17. A. Michels and C. Michels, *Proc. Roy. Soc.* **A153**:214 (1936).
18. D. R. McGregor, J. C. Holste, P. T. Eubank, K. N. Marsh, and K. R. Hall, *Fluid Phase Equil.* **35**:153 (1987).
19. C. Tsonopoulos, *AIChE J.* **20**:263 (1974).
20. K. S. Pitzer and R. F. Curl, *J. Am. Chem. Soc.* **79**:2369 (1957).
21. A. Abbaci, H. R. van den Berg, E. Sakonidou, and J. V. Sengers, *Int. J. Thermophys.* **13**:1043 (1992).
22. G. X. Jin, S. Tang, and J. V. Sengers, *Fluid Phase Equil.* (in press).
23. R. B. Griffiths and J. C. Wheeler, *Phys. Rev.* **A2**:1047 (1970).
24. W.-W. Lau, Ph.D. dissertation (Texas A&M University, College Station, Dec. 1986). (Available through University microfilms, Ann Arbor, MI.)
25. D. R. Friend, NIST Standard Reference Database 14, Version 9.08 (1992).